Investigating In-Route Energy Consumption Profiles of Battery-Electric Buses Using Open-Source Transportation Simulation

Yexuan Gao
Department of Engineering Science
University of Oxford
Email: sabrinayxg@gmail.com

David C. H. Wallom
Department of Engineering Science
University of Oxford
Email: david.wallom@oerc.ox.ac.uk

Abstract

In the context of ambitious net-zero targets and decarbonisation of transport, bus fleet electrification has emerged as a likely significant transformation. This study proposes a multi-step model for investigating the effect of route structure on electric buses' energy consumption. Initial bus fleets were selected based on the route demand and characteristics, using a Multi-Criteria Decision Matrix. Energy consumption modelling of buses was differentiated into auxiliary and powertrain components to consider select operational characteristics. Travel flow analysis was conducted using the Simulation of Urban Mobility (SUMO) software through importing transport networks, defining bus stop locations and routes. A case study of Oxfordshire's existing bus system was conducted given worst-case seasonal temperatures including optimized electric bus selection for five selected routes, and a flow simulation to determine the energy consumption patterns of different route types.

Powertrain modelling showed strong monotonic relationships between route length and propulsion energy consumption, ranging from 19.1 kWh to 105 kWh for the shortest and longest routes respectively. Higher levels of congestion, proxied through average inter-stop speeds, correlated with lower instantaneous energy increases. Overall, auxiliary systems constituted a maximum of 11% of total energy consumption across all routes simulated. Auxiliary system modelling also showed that total energy consumption and the proportion spent on auxiliary services were only weakly influenced by route length; instead, stronger correlations were observed with the total number of stops, due to a significant impact on door opening times. Future work could investigate the optimised location of depot and in-route charging infrastructure to best support electric bus fleets considering additional constraints of grid congestion. These findings contribute to research on the infrastructural needs of a zero-carbon bus fleet by providing local authorities with a high-level understanding of e-bus energy demands across the region.

Introduction

In the face of the urgent climate crisis, numerous countries globally are pursuing rapid decarbonisation strategies to meet national and international targets. The transport sector is of notable importance; to tackle citizens growing mobility requirements, governments have begun ramping up innovations in sustainable transport infrastructure with public mobility options being a key solution. Public transport, such as buses, offer multiple benefits of increased fuel efficiency and decreased traffic congestion, in addition to crucial social equity benefits such as reducing the financial burden of transport expenditure in low-income families, expanding spatial access to opportunities, and localised economic rejuvenation in connected communities[1]. Electrically chargeable vehicles are rising as dominant decarbonising technologies in the alternative-fuel subsector, increasing in market share by 170% from 2018-19 to make up 4% of newly registered buses in the European Union[2]. Government institutions in developed nations like the UK and Netherlands have all set major targets towards bus fleet electrification, concurrently as rapidly growing countries like India have accounted for 25% of all global e-bus orders in 2018 excluding China[3].

[1] E. Blumenberg, "Social Equity and Urban Transportation," in The Geography of Urban Transportation, 4th ed., G. Giuliano and S. Hanson, Eds. Guilford Publications, 2017.
[2] "Medium and Heavy Buses (over 3.5t): New Registrations by Fuel Type in the European Union for 2019," Apr. 2020. Accessed: Jun. 08, 2021. [Online].
[3] "Indian electric bus market, what's going on?," Sustainable Bus, Oct. 05, 2018.

Nevertheless, strides towards greater fleet electrification have been constrained by concerns around e-bus energy consumption and range, as many public transport operators manage long-haul routes spanning rural and urban regions that may be hard to decarbonise. The relationship between route parameters and energy consumption profiles posits an interesting question, as variables such as stopping and acceleration frequency, road types, and traffic congestion all impact e-bus motors' energy consumption. This is additional to the power consumption of auxiliary systems, of which heating, ventilation, and air conditioning (HVAC) are energy-intensive processes required for passenger thermal comfort. Such systems see further uncertainty in power consumption profiles due to seasonal weather profiles, alongside route-dependent variables like door openings and thermal emissions.

This study thereby investigates how e-buses' energy consumption profiles are affected by both route characteristics and external weather conditions. Official standards from the United Nations Economic Commission for Europe were adopted, which technically specifies a bus as 'vehicles designed and constructed for the carriage of passengers, having more than eight seats with maximum mass either not exceeding (M2 category) or exceeding (M3 category) 5 tonnes'[4]. Only electricity-powered buses were considered for in-route energy consumption through transport flow analysis.

Background

Bus Fleet Operations

Several categories of bus routes were identified to ensure that applications of route modelling can employ a representative sample of route types. Whilst the overall energy consumption model can be applied for all bus routes, an overview of various route types can allow local authorities to develop indicative insights into route characteristics broadly relating to energy consumption profiles. Whilst no standard terminology was identified across planning authorities, this study considers several main categories – end-to-end radial and non-radial routes, and looped routes. An indicative representation of each route type is shown in Figure 1.

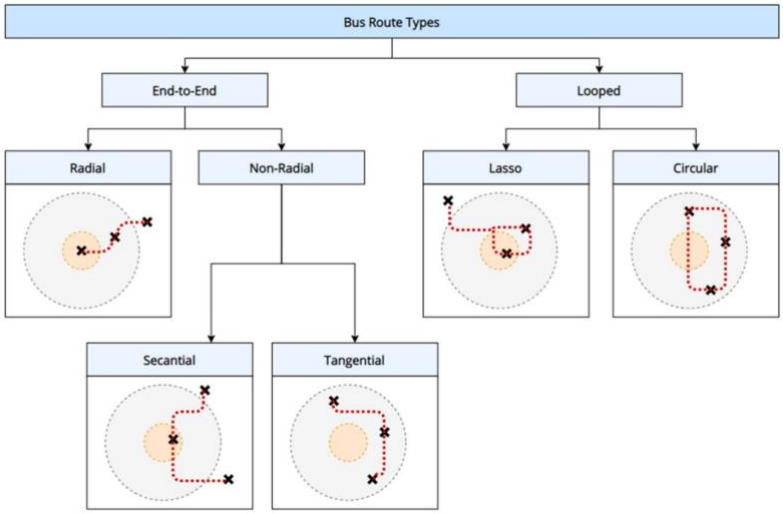

Figure 1: Geometric categorisation of bus route types

Bus Selection Optimisation

As fleet electrification becomes increasingly likely, there is the impetus for bus operators to make informed procurement decisions and trade-offs based on bus and route characteristics. Multicriteria decision analysis has been proposed by M. Hamurce et. al[5] in e-bus selection utilising analytical hierarchy process (AHP) and technique for order preference by similarity to ideal solution (TOPSIS). Due to its inherent simplicity, AHP has been adopted in a variety of settings requiring decision-making attributes spanning social, economic, technical, and other dimensions. Expanding upon pure electric options, J. Ribau et. al[6] proposed a holistic method to simultaneously compare different alternative fuel buses: battery-electric, fuel cell hybrid, and plug-in hybrid. To ensure that identified parameters were most useful to operators, J. Gong et. al[7] proposed a data-based road-testing approach

[4] "Consolidated Resolution on the Construction of Vehicles (R.E.3) Revision 6," Jul. 2017. Accessed: Jun. 09, 2021. [Online]. Available: https://unece.org/fileadmin/DAM/trans/main/wp29/wp29resolutions/ECE-TRANS-WP.29- 78r6e.pdf.

[5] M. Hamurcu and T. Eren, "Electric bus selection with multicriteria decision analysis for green transportation," Sustainability (Switzerland), vol. 12, no. 7, Apr. 2020, doi: 10.3390/su12072777.

[6] J. P. Ribau, S. M. Vieira, and C. M. Silva, "Selecting sustainable electric bus powertrains using multi-preference evolutionary algorithms," International Journal of Sustainable Transportation, vol. 12, no. 8, Sep. 2018, doi: 10.1080/15568318.2017.1418464.

[7] J. Gong et al., "Road Test-Based Electric Bus Selection: A Case Study of the Nanjing Bus Company," Energies, vol. 13, no. 5, Mar. 2020, doi: 10.3390/en13051253.

investigating factors that most significantly affect bus selection. Instead of computer test bench simulations, a two-month road-based testing was implemented to better reflect real-world operational properties.

Energy Consumption Evaluation

To determine the factors influencing e-bus energy consumption, three main methods have been employed in literature: white-box, black-box, and grey-box models[8]. White-box methods are standardised, equation-based analytical methods using bottom-up evaluation of physical and chemical processes, while black-box methods utilise pure data-driven models from large amounts of real-world operation data. For brevity, in this section, grey-box methods are not discussed explicitly but rather amalgamated with other data-driven approaches.

White-Box Energy Modelling

Propulsion Systems

White-box, analytical energy consumption models rely on a detailed understanding of e-buses' physical and chemical processes to build a bottom-up model from each system subcomponent. These methods are typically also referred to as longitudinal dynamics models (LDMs), as general principles of mechanics are used to derive the movement behaviour of vehicles along their longitudinal direction[9]. A 2021 review of EV modelling techniques disaggregated analytical methods into microscopic and macroscopic scales respectively – the former referring to models that generate energy consumption estimates for individual EVs at high frequency, whilst the latter examines the influence of driving characteristics at aggregated spatial or temporal spans[10]. The share of macroscopic models in academic literature has consistently increased since 2011; they are particularly useful for investigating the relationship between EV energy consumption and geometry attributes, although macroscale models often use traffic factors as a proxy for detailed vehicle dynamics[11].

Several of these variables were configured for an e-bus by A. Ritari et. al[12] in a quasi-static numerical computational model through calculation flows beginning from the driving cycle to the inverter – through traffic or environment-related conditions were not explicitly considered. Regression modelling of urban e-buses in southern China[13] showed the significance of non-vehicular factors: high congestion and hot summer temperatures both led to reduced battery performance, leading to higher observed efficiencies during night-time or mild cooler seasons. Methods where HVAC and auxiliary systems are modelled independently from the main propulsion system, have additionally allowed for energy consumption simulation under different operating conditions including weather and passenger loading[14]. Notably, these methods require a detailed, specific understanding of components to determine accurate simulation results.

Auxiliary Systems

Non-traction auxiliary energy consumption contributes a significant proportion of total energy use and thus the feasibility of e-buses is highly sensitive to auxiliary system efficiency. Analytical models can decompose and incorporate operational variables such as door opening times, ventilation efficiencies, and temperature differences that are not captured by fixed performance factors offered by manufacturers. Basic auxiliary functions are typically categorised as thermal and non-thermal – the former includes heating, ventilation, and air conditioning (HVAC) systems, whilst the latter includes various mechanical or drive support systems.

A detailed thermal model for electric and hybrid vehicles proposed by H. Basma et. al[15] considered four main forms of heat transfer between the interior and ambient environment: convection, radiation, transmission, and absorption through glazing and internal cabin materials. Whilst highly detailed, almost 40 variables were required for full model functioning, and sensitivity analyses showed that some variables had much stronger impacts on final energy consumption results than others. This suggests a practical trade-off between model fidelity and complexity

[8] M. Zhou, H. Jin, and W. Wang, "A review of vehicle fuel consumption models to evaluate eco-driving and eco-routing," Transportation Research Part D: Transport and Environment, vol. 49, pp. 203–218, Dec. 2016, doi: 10.1016/j.trd.2016.09.008.

[9] J. Asamer, A. Graser, B. Heilmann, M. Ruthmair, and M. Ruthmair, "Sensitivity analysis for energy demand estimation of electric vehicles," Transportation Research Part D, vol. 46, pp. 182–199, 2016, doi: 10.1016/j.trd.2016.03.017.

[10] Y. Chen, G. Wu, R. Sun, A. Dubey, and A. Laszka, "A Review and Outlook of Energy Consumption Estimation Models for Electric Vehicles," SAE International Journal of Sustainable Transport., Energy, Environment, & Policy, vol. 2, no. 1, pp. 79–96, 2021, doi: https://doi.org/10.4271/13-02-01- 0005.

[11] Masikos Michail, Demestichas Konstantinos, Adamopoulou Evgenia, and TheologouMichael, "Mesoscopic forecasting of vehicular consumption using neural networks," Soft Computing - A Fusion of Foundations, Methodologies and Applications, vol. 19, no. 1, pp. 145–156, Jan. 2015, doi: 10.1007/S00500-014-1238-4.

[12] A. Ritari, J. Vepsäläinen, K. Kivekäs, K. Tammi, and H. Laitinen, "Energy Consumption and Lifecycle Cost Analysis of Electric City Buses with Multispeed Gearboxes," doi: 10.3390/en13082117.

[13] S. Wang, C. Lu, C. Liu, Y. Zhou, J. Bi, and X. Zhao, "Understanding the Energy Consumption of Battery Electric Buses in Urban Public Transport Systems," Sustainability 2020, Vol. 12, Page 10007, vol. 12, no. 23, Nov. 2020, doi: 10.3390/SU122310007.

[14] H. Basma, C. Mansour, M. Haddad, M. Nemer, and P. Stabat, "Comprehensive energy modeling methodology for battery electric buses," Energy, vol. 207, p. 118241, Sep. 2020, doi: 10.1016/J.ENERGY.2020.118241.

[15] H. Basma, C. Mansour, M. Haddad, M. Nemer, and P. Stabat, "Comprehensive energy modeling methodology for battery electric buses," Energy, vol. 207, p. 118241, Sep. 2020, doi: 10.1016/J.ENERGY.2020.118241.

should be considered for the technical capabilities of local authorities. Recent work by O. Hjelkrem et. al[16] offered a moderately detailed approach to dissecting auxiliary energy consumption in e-buses – thermal performance was defined with variables of vehicle speed and ventilation rates, and door opening times at each stop. Through field verification, auxiliary energy estimations were shown to be accurate on a trip-level basis with a tendency for underestimation in higher-temperature scenarios beyond 30°C. Altogether, auxiliary systems contributed up to 44% of total energy consumption, confirming the importance of including these system operations in energy analyses.

Traffic Flow Simulation

Open-source traffic simulation software, typically agent-based, offer the advantage of visual simulation with existing route parameters and traffic flow alongside other vehicle agents. Additionally, route-based simulation allows for the generation of drive cycles that can be adapted to achieve other objectives such as air pollutant or greenhouse gas emissions modelling at an individual route level. Three open-source software – MATSim (Multi-Agent Transport Simulation), TRANSIMS (TRansportation ANalysis and SIMulation System), and SUMO (Simulation of Urban MObility) had been systematically evaluated by D. Allan et. al[17] for their utility in transport electrification modelling. Notably, MATSim does not characterise energy consumption by acceleration, a major drawback as user driving and braking patterns have significant impacts on final energy use. Whilst TRANSIMS share common capabilities as SUMO, existing documentation is more complete for SUMO and is a crucial advantage to allow for simulation scalability and ease of adoption. Nevertheless, all three software are currently unable to incorporate power infrastructure constraints such as transmission networks and grid congestion points, limiting their standalone efficiency in charging deployment evaluation with DSOs.

In SUMO, traffic flow and infrastructure conditions on a micro-level can be readily imported and edited as a network configuration, and external influences such as traffic congestion can further be inspected. As this study is principally concerned with examining the varying energy consumption of different route types rather than the absolute consumption profile of any route, it is therefore assumed that SUMO, as a flow-based software, offers a more representative and usable tool for local operators. The SUMO energy model adopts a white-box approach to determining battery energy state at each time step with explicit considerations for variations in driving energy profiles due to route geometries. For a given route and topographic profile, SUMO's energy model was able to achieve a least-squared error of 3.4 kWh^2 at a discrete time step of 1 s[18]. However, SUMO has limited accuracy when compared to real-world experimental results with up to 11% battery state-of-charge error for European driving cycles[19]. This is primarily due to lacking considerations of external ambient temperature effect on auxiliary power consumption – energy modelling errors increase with experimental conditions set at 35°C and -7°C, as opposed to a standard 25°C. Suggestions of auxiliary power consumption as a function of external temperature have been recommended to increase SUMO modelling accuracy: however, in the context of this study focusing on the effect of route types on varying energy consumption, they have not been implemented. Rather, auxiliary system energy consumption was determined for worst-case weather conditions to assist in transport planning at a lower level of complexity.

Methodology

Bus Fleet Selection

To optimise for e-buses based on routes, a multi-criteria decision-making and AHP-TOPSIS method was adopted. Unlike other methods reviewed from the literature, this approach can handle complex and field-specific decision attributes through basic pairwise comparisons easily deployable in local authorities. Whilst scalability may come at the expense of detail and weighting accuracy, this is a useful high-level tool that complements traffic flow modelling to provide an overview of energy consumption profiles across various route types.

Adapting from previous studies, four main decision criteria were prioritised from available bus technical specification datasheets. These are seating capacity (C1), maximum power output (C2), maximum energy storage capacity (C3), and charging/refuelling rate (C4), as presented in Table 1. Seating capacity broadly correlates to the overall capacity, including the permissible number of standing passengers which are often unspecified in manufacturers' specifications. Maximum power output broadly relates to bus travel speed. Maximum energy

[16] O. A. Hjelkrem, K. Y. Lervåg, S. Babri, C. Lu, and C. J. Södersten, "A battery electric bus energy consumption model for strategic purposes: Validation of a proposed model structure with data from bus fleets in China and Norway," Transportation Research Part D: Transport and Environment, vol. 94, p. 102804, May 2021, doi: 10.1016/j.trd.2021.102804.

[17] D. F. Allan and A. M. Farid, "A Benchmark Analysis of Open Source Transportation-Electrification Simulation Tools," in IEEE Conference on Intelligent Transportation Systems, Proceedings, ITSC, Oct. 2015, vol. 2015-October, pp. 1202–1208, doi: 10.1109/ITSC.2015.198.

[18] T. Kurczveil and E. Schnieder, "Implementation of an Energy Model and a Charging Infrastructure in SUMO," in 1st SUMO User Conference, May 2013, pp. 88–94, Accessed: Jun. 12, 2021. [Online].

[19] I. Sagaama, A. Kchiche, W. Trojet, and F. Kamoun, "Evaluation of the Energy Consumption Model Performance for Electric Vehicles in SUMO," Oct. 2019, doi: 10.1109/DS-RT47707.2019.8958704.

storage capacity, generalised to incorporate both e-bus battery storage and diesel fuel tanks in hybrid buses, broadly correlates to the driving range and how often refuelling or recharging might be required. Charging rates are specific to e-buses and obtained from manufacturers' specification sheets; hybrid buses were estimated with a refuelling rate based on that of conventional diesel buses of 600 l per minute. Considering the energy density of diesel at a typical 9.7 kWh/l, this corresponds to a 21 MW refuelling rate and was assumed constant for all hybrid buses; power charging rates for hybrid buses were not considered. In the AHP-TOPSIS bus fleet selection process, a confidence ratio of 10% was used for the pairwise comparisons of eigenvectors.

Table 1. Technical specifications of selected electric and hybrid buses

Specification	**Full Electric**					**Diesel-Electric Hybrid**	
	Volvo-7900 (12)	Yutong Pelican E12	BYD K9	Mercedez eCitaro G4	Volvo-7900 (18)	Enviro400ER	Scania K320 UB 4X2
Dimensions (m), L×W×H	12.0×2.6×3.3	12.0×2.6×3.3	12.0×2.6×3.4	18.0×2.6×3.4	18.0×2.6×3.3	11.0×2.6×4.3	11.0×2.6×3.2
Seat capacity	35	40	35	41	50	67	42
Maximum power output (kW)	160	200	300	250	400	195	235
Energy storage capacity (kWh)	200	422	324	396	300	1,961	2,444
Charging rate (kW)	300	150	80	450	450	21,000*	21,000*
** A 'charging' rate of 21MW was assumed for diesel-electric hybrids corresponding to the energy density of diesel fuel.*							

Route Simulation

Distances between bus stops for routes were sourced from Google Maps, whilst the schedule for each stop was obtained from Google Maps and cross-referenced against Moovit. For scheduling consistency and to ensure similar congestion modelling where relevant, all routes used an 8:30am start time as a default unless otherwise unavailable. This allowed the average velocity between each bus stop to be found.

To simulate the transport flow of future e-bus fleets, SUMO was identified as the most suitable opensource software. Within SUMO, existing road infrastructure can be imported from OpenStreetMap (OSM) using the Python-based OSM Web Wizard. This allows geospatial data from a predefined area to be extracted from OSM and saved directly as a net.xml file, which can be edited in the netedit application. Edges were defined with the appropriate speed limits, which are the average velocities of buses travelling between each bus stop. A separate route file must then be written in .xml to specify bus characteristics as well as edges along each bus route. Thereafter, a SUMO configuration file must be written to amalgamate all three files (network, additionals, and route) into a single simulation of filetype .sumocfg, and include written code specifying the type of output files required to be generated from the simulation. For this study, the main output used was battery-output for the vehicle, whilst trip-info and stop-output were also generated to review the route travelled during simulation.

Energy Consumption Modelling

Propulsion Systems

SUMO's energy model adopts the following overarching white-box approach to determine the in-route energy consumption of vehicle agents, where the energy state of a vehicle at discrete time step k is defined by the sum of its kinetic, potential, and rotational energy. As the vehicle progresses along its route, the difference in energy states across two timesteps can be defined as the sum of energy gains and losses throughout the journey. The energy loss term is defined as the sum of energy loss from air resistance, rolling resistance, curve resistance, and constant power consumption from secondary auxiliary functions.

The energy gain term is obtained through the difference in energy states and is scaled by user-defined efficiency values to determine battery energy change. Recuperation efficiency (η_{recup}) is the constant efficiency factor for regenerative energy applied when there is a positive energy gain term ($\Delta E_{\text{gain}[t]} > 0$), whilst propulsion efficiency (η_{prop}) is the constant efficiency factor for propulsion motion applied when there is a negative energy gain term ($\Delta E_{\text{gain}[t]} < 0$). As such, overall variation in battery energy during movement can be summarised as in Equation 1.

Equation 1. SUMO battery energy consumption model

$$E_{batt}[t+1] - E_{batt}[t] = \begin{cases} \Delta E_{gain}[t] \cdot \eta_{recup} & , if\ \Delta E_{gain}[t] > 0 \\ \Delta E_{gain}[t] \cdot \eta_{prop} & , it\ \Delta E_{gain}[t] < 0 \end{cases}$$

Auxiliary Systems

To model energy consumption from auxiliary systems, the model developed by O. Hjelkrem et. al was adapted given its validated performance against real-world results and reasonable input data requirements. A worst-case performance was considered to enable appropriate battery sizing to accommodate all operational conditions. Overall, auxiliary system power consumption can be summarised as in Equation 2.

Equation 2. Auxiliary system power consumption

$$P_{aux} = P_{heating/cooling} + P_{ventilation} + P_{other}$$

Power for other operating systems (P_{other}) includes devices such as interior lighting and secondary motion systems including steering and pneumatic braking support subsystems. As there is little explicit reference to these systems in literature, the upper-bound value of 3 kW from O. Hjelkrem et. al was used for a worst-case assumption. Power for ventilation ($P_{\text{ventilation}}$) refers to the power required to drive air through the ventilation system and is affected by factors including the location of air vents and duct flow design. Whilst most manufacturers do not disclose a disaggregated HVAC power consumption analysis, the Thermo King TE15 HVAC system supplied for xcelsior's Charge NG e-bus model was referenced, which had an approximate ventilation capacity of 3,800 cubic feet (108 cubic meters) per minute[20]. Considering an air pressure difference of 140 Pa as observed in real-world operational buses[21], this results in a ventilation system power rating of 0.25 kW. A more conservative estimate of 0.5 kW was assumed for this study considering trends towards higher ventilation rates post-COVID-19.

Power for heating and cooling ($P_{\text{heating/cooling}}$) can further be defined in Equation 3 where $\rho = 1.2 kg/m^3$ refers to the density of air, $c_{\text{p}} = 1.005$ refers to the specific thermal capacity of air, Q_{vent} and Q_{doors} refer to the volume of air exchanged per second from ventilation and door-opening respectively, $H_{\text{doors}} = 0, 1$ is a Heaviside step function defining whether bus doors are open ($H_{\text{doors}} = 1$) or closed ($H_{\text{doors}} = 0$), and ΔT refers to the temperature difference between bus interior and external ambient environment.

Equation 3. Power consumption of heating and cooling functions

$$P_{heating/cooling} = \rho \cdot c_p \cdot (Q_{vent} + Q_{doors} \cdot H_{doors}) \cdot |\Delta T|$$

Notably, Q_{vent} can be found by considering the air change rates of internal bus systems, defined as the number of times per hour that all the air within an internal volume of the building is replaced. An experimental study of three Californian bus systems found that air changes rates could vary substantially between 3 to 9 per hour depending on whether windows were open or closed[22]. It is useful to also consider the context of post-COVID-19 responses – the European Centre for Disease Prevention and Control recommended broad actions to increase the air change and ventilation rates of indoor spaces to reduce the transmission risk of airborne viruses for all member states [23], whilst the UK CIBSE regulations encourage a minimum air change rate of 5 per hour for indoor spaces [24]. Local authorities should consider contextual behavioural factors to determine reasonable estimates for Q_{vent}: for instance, in regions where air-conditioning is prevalent and windows are fully closed during summer operational periods, a low air change of 3- 5 per hour may be assumed. For a given air change rate (ACR), Q_{vent} can be found via Equation 4 where V_{bus} refers to internal bus volume.

Equation 4. Rate of volumetric air exchange for ventilation

$$Q_{vent} = V_{bus} \times \frac{ACR}{3600}$$

Air exchanges due to door activity Q_{doors} can be further dissected into two contributing factors: Q_{orifice} and $Q_{\text{passengers}}$, referring to direct air flow from the door opening and from the air flow from passenger activity, respectively, in Equation 5. Q_{orifice} can be defined by the following gravity-driven flow relationship[25] where k refers to the orifice coefficient, A_0 and H refer to door area and height respectively, and g' refers to the effective acceleration of gravity. For normal doorways, k ranges from 0.4 to 0.6 – it is assumed that this range of values can be reasonably extended for bus doorways.

Equation 5. Rate of volumetric air exchange due to flow through door orifice

[20] "Thermo King T Series Specifications."

[21] K. Nikam and S. Borse, "Study of Air Flow through a Open Windows Bus Using OpenFOAM," International Journal of Fluids Engineering, vol. 6, no. 1, pp. 53–64, 2014, Accessed: Aug. 06, 2021. [Online].

[22] S. K. Chaudhry and S. P. Elumalai, "The influence of school bus ventilation scenarios over in-cabin PM number concentration and air exchange rates," Atmospheric Pollution Research, vol. 11, no. 8, pp. 1396–1407, Aug. 2020, doi: 10.1016/j.apr.2020.05.021.

[23] European Centre for Disease Prevention and Control, "Heating, ventilation, and air-conditioning systems in the context of COVID-19: first update" Nov. 2020. Accessed: Jul. 01, 2021. [Online] https://www.ecdc.europa.eu/sites/default/files/documents/Heating-ventilation-air-conditioning-systems-in-the-context-of-COVID-19-first-update.pdf

[24] CIBSE, "Ventilation in Buildings (webpage)" May 2015. Accessed: Jul. 01, 2021. [Online] https://www.cibse.org/knowledge/knowledge-items/detail?id=a0q20000006oamlAAA

[25] D. J. Wilson and D. E. Kiel, "Gravity driven counterflow through an open door in a sealed room," Building and Environment, vol. 25, no. 4, pp. 379–388, Jan. 1990, doi: 10.1016/0360-1323(90)90012- G.

$$Q_{orifice} = \frac{k}{3} \cdot A_0 \cdot \sqrt{g'H}$$

Air exchanges due to passenger activity can be defined by Equation 6 proposed in an experimental study investigating airflow in hinged and sliding doors[26], where $\dot{\eta}$ refers to the rate which passengers leave or board at each bus stop, and Vpassenger refers to the volume of air exchanged due to the motion of each passenger.

Equation 6. Rate of volumetric air exchange due to passenger motion

$$Q_{passengers} = \dot{\eta} \cdot V_{passenger}$$

It was found that the normalised air volume exchanges due to passenger movements ($V_{\text{passenger}}$) were 0.25 for sliding doors and 0.75 for hinged doors operating at an hourly air change rate of 6[27]. Whilst the performance of folding bus doors has not been explicitly studied in the literature, it is reasonable to make a worst-case assumption that this more closely resembles the performance of hinged door openings.

Oxfordshire Case Study

To apply the discussed methodology, Oxfordshire was selected as a case study site. Oxford City, alongside Coventry, are set to become the UK's first all-electric bus cities, receiving up to £50 million (€59 million) in government grants to demonstrate technically, socially, and economically feasible plans for electric bus fleet rollouts[28]. The county has a relatively simple bus network, predominantly serving residents through six radial corridors from the city centre. Additionally, Oxfordshire is the least densely-populated county in southeast England – the ability for e-buses to operate concurrently in spacious rural regions and dense Oxford City will be crucial to scaling e-bus adoption in the county and beyond. The Oxfordshire Local Transport Plan 2011-2030 also identified increasing centralisation of services as a hurdle to access in rural regions, worsening isolation of vulnerable groups[29].

The major bus operators within Oxfordshire are Stagecoach and the Go-Ahead Group, the latter of which runs both the Oxford Bus Company and Thames Travel services; both operators' services overlap on all six main corridors spanning from Oxford City. In 2021, both Stagecoach and the Go-Ahead Group have committed publicly to a zero-emission bus fleet by 2035 [30] [31] although supporting strategy roadmaps for achieving these targets are yet to be published.

Bus Fleet and Routes Selection

To inform bus route selection for modelling, commuting data from Oxfordshire County Council's Joint Strategic Needs Assessment was referenced. This dataset based on the latest 2011 Census showed that Oxford City received the greatest net inflow of commuters at 29,839 annually for work[32] – of these, journeys by bus, minibus, or coach made up 17.6% of total mode share[33]. The most common origins for travel into Oxford City were internally from Oxford (55.0%), followed by Abingdon (6.1%) and Kidlington (5.8%). To incorporate a social equity dimension, it was further noted that despite being one of the most affluent areas in the UK, Oxfordshire contained 10 wards within the top 20% most deprived in England as of 2020[35]. The County's Annual Public Health Report showed that seven of these wards were located within 10 miles (16 kilometers) of Oxford – including Rose Hill and Iffley, Blackbird Leys, Abingdon, and Littlemore[34]. As such, route selection is aimed to maximise inclusion of both the most common trip destination trends, as well as deprived communities currently served by public buses. A total

[26] P. Kalliomäki, P. Saarinen, J. W. Tang, and H. Koskela, "Airflow patterns through single hinged and sliding doors in hospital isolation rooms – Effect of ventilation, flow differential and passage," Building and Environment, vol. 107, pp. 154–168, Oct. 2016, doi: 10.1016/j.buildenv.2016.07.009.

[27] P. Kalliomäki, P. Saarinen, J. W. Tang, and H. Koskela, "Airflow patterns through single hinged and sliding doors in hospital isolation rooms – Effect of ventilation, flow differential and passage," Building and Environment, vol. 107, pp. 154–168, Oct. 2016, doi: 10.1016/j.buildenv.2016.07.009.

[28] "Coventry and Oxford set to be UK's first all-electric bus cities," GOV.UK, Jan. 06, 2021.

[29] "Oxfordshire Local Transport Plan 2011-2030: Rural Areas," Oxford, Apr. 2012. Accessed: Jun. 18, 2021. [Online]. Available: https://www2.oxfordshire.gov.uk/cms/sites/default/files/folders/documents/roadsandtransport/transportpoliciesandplans/localtransportplan/ltp3/26-ruralareas.pdf.

[30] M. Griffiths, "Financial Report: Preliminary Results for Year Ending 1 May 2021," Jun. 2021. Accessed: Jul. 01, 2021. [Online]. Available: https://www.stagecoachgroup.com/~/media/Files/S/StagecoachGroup/Attachments/media/publication-financial-reports/preliminary-results-30th-june-2021.pdf.

[31] "Investment in environmentally-friendly buses," The Go-Ahead Group. https://www.go-ahead.com/sustainability/case-studies/investment-environmentally-friendly-buses (accessed Jul. 01, 2021).

[32] "Travelling to work: commuting patterns in Oxfordshire," Oxford, Sep. 2014. Accessed: Jun. 22, 2021. [Online]. Available: https://insight.oxfordshire.gov.uk/cms/system/files/documents/TTW%20briefing_110914_FINAL. pdf.

[33] "Settlement-based journey-to-work destinations," Oxfordshire Insight, 2011. https://public.tableau.com/views/2011CensusTTWDestinationSettlementGL/LAleveljourneyorigin s?:embed=y&:showVizHome=no (accessed Jun. 22, 2021).

[34] A. Azhar, "Some are more equal than others: Hidden inequalities in a prospering Oxfordshire," Oxford, May 2020. Accessed: Jun. 22, 2021. [Online]. Available: https://www.oxfordshire.gov.uk/sites/default/files/file/publichealth/PublicHealthAnnualReportMay2020.pdf.

of five bus routes were selected, as shown in Table 2, involving two bus operators – Stagecoach and the Go-Ahead Group.

Table 2. Selected Oxfordshire bus routes for energy modelling

Service	Operator	Coverage	Stops	Rationale for Selection
S4	Stagecoach	Banbury – Oxford City Centre	60	Radial to the city centre, longest route for operator
3A	Oxford Bus Company	Oxford City Centre – Cowley	46	Radial to the city centre, passes through several deprived regions
233	Stagecoach	Burford – Woodstock	39	Non-radial, passes through high-traffic regions
33	Thames Travel	Wallingford – Abingdon	36	Non-radial, passes through 3 terminal hubs
400	Oxford Bus Company	Seacourt P&R – Thornhill P&R	13	Non-radial P&R route, passes through the city centre

Bus fleet selection was optimised for each route considering the demands for each bus routeThese routes were differentiated broadly because S4 and 3A are longer routes and may hence require greater range and passenger-carrying capacities to ensure minimal disruptions to existing schedules. As routes 233, 33, and 400 are relatively shorter or do not travel directly through congested central areas, they are assumed to be less demanding on the range and instead prioritising maximum output power. Following this pairwise criteria priorisation and solving the corresponding eigenvector problem,two different sets of weights were generated for services S4 and 3A, and 233, 33, and 400 respectively. Both sets of weighting results and confidence ratios (CRs) are presented in Table 3.

Table 3. Weighting results for each criterion, differentiated by route category

Routes	Seat capacity	Maximum output power (kW)	Energy storage capacity (kWh)	Charging or refuelling rate (kWh)
S4, 3A (CR=7.8%)	0.120	0.106	0.427	0.348
233, 33, 400 (CR=6.7%)	0.091	0.570	0.093	0.247

Both e-buses and hybrid models were considered in the initial round of weighting to determine the optimum low-emission technology to serve each route's needs. The same process was also repeated but only for e-bus options to determine the technical specifications to be input into the energy modelling simulation. Hybrid and e-bus results for routes S4 and 3A are shown in Table 4, whilst results for routes 33, 233, and 400 are shown in Table 5. Both hybrids and e-buses were included in this weighting step to assess whether hybrids offer significant benefits over e-buses for specific routes. As observed by their higher relative closeness values, routes with greater length (S4 and 3A) were better suited for hybrids which allow for greater range – this benefit was less prominent when considering shorter routes that do not pass through congested central areas (33, 233, 400). Nevertheless, only the optimum e-bus results, omitting hybrids, were used for energy consumption modelling in the later steps. As such, routes S4 and 3A were modelled with bus fleets following technical specifications from the Mercedez eCitaro G4, whilst routes 33, 233, and 400 were modelled with that from the Volvo-7900 (18).

Table 4. Matrix of relative closeness values for routes S4 and 3A, hybrids and e-buses

Results	Volvo-7900 (12)	Yutong Pelican E12	BYD K9	Mercedez eCitaro G4	Volvo-7900 (18)	Enviro400ER	Scania K320
Hybrid and E-Buses	0.016	0.081	0.081	0.067	0.117	0.825	0.913
E-Buses Only	0.410	0.467	0.291	0.795	0.738	-	-

Table 5. Matrix of relative closeness values for routes 33, 233, and 400, hybrids and e-buses

Results	Volvo-7900 (12)	Yutong Pelican E12	BYD K9	Mercedez eCitaro G4	Volvo-7900 (18)	Enviro400ER	Scania K320
Hybrid and E-Buses	0.099	0.206	0.426	0.025	0.569	0.517	0.599
E-Buses Only	0.252	0.271	0.518	0.320	0.952	-	-

Energy Consumption Modelling

Propulsion Systems

Travel time data was obtained from Google Maps' scheduling tool during Monday AM peak hours, defined by the Oxfordshire County Council as between 7:30 am and 9:30 am[35]. Where average bus speeds were found to be larger than 50 km/h, an absolute maximum speed of 50 km/h was applied instead. Considering the variations in speed distributions and stop locations, propulsion energy consumption was modelled through geolocation and speed data inputs in SUMO. Total respective route lengths and propulsion energy consumption are shown in Table 6.

Table 6. Summary of respective route lengths and propulsion energy consumption

Route	S4	3A	233	33	400
Length (km)	43.2	18.5	27.9	24.5	9.3
Propulsion Energy Consumption (kWh)	105.0	56.5	83.0	54.2	19.1

Overall, route length correlates strongly with aggregate propulsion energy consumption – with the minor exception of routes 33 and 3A, propulsion energy increases monotonically with route length. This affirms that on a macro-scale, route length is the largest determinant of propulsion energy consumption although traffic conditions will further influence energy profiles on a localised scale.

Correlating the energy consumption timestamp with buses' in-route location, plateaus are found to correlate with journeys in heavily congested areas where bus speeds are extremely slow. For instance, the relatively flat profile between 1311-1599 seconds in Route 233 corresponds to the path between Holloway Road and Market Square in Witney, where average bus speeds are stalled to 3.6 km/h. This is demonstrated in Figures 2 and 3.

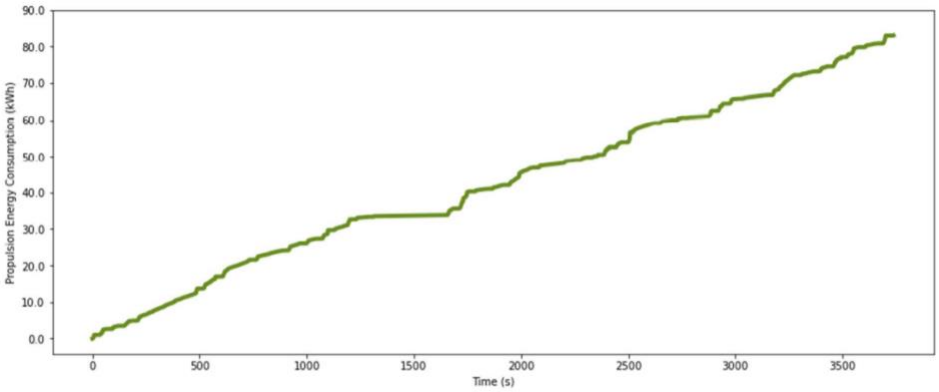

Figure 2: Route 233 propulsion energy consumption

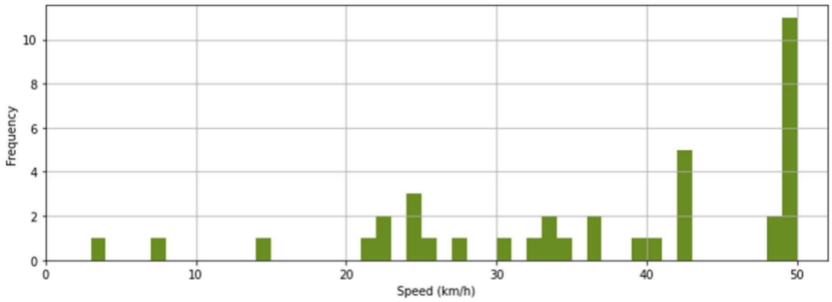

Figure 3: Route 233 speed distribution

The traffic simulation demonstrates that propulsion energy consumption is closely interlinked with overall congestion and average vehicle speeds, reaffirming the sensitivity of bus energy profiles to changes in traffic conditions. Practically, this means that operators must have a clear understanding of in-route traffic conditions to accurately determine the necessary battery capacities of fleet e-buses and location of various charging infrastructure. Such an understanding can be strengthened through partnership with local authorities, who establish and monitor legislation including Low Traffic Neighbourhoods that can significantly influence expected congestion levels.

[35] "Oxfordshire A and B Road Town Congestion Maps," 2015. Accessed: Jul. 22, 2021. [Online]. Available: https://www2.oxfordshire.gov.uk/cms/sites/default/files/folders/documents/roadsandtransport/tra ffic/AnnualTownCongestionReport.pdf.

The specific and total energy consumption for each route is presented in Figure 4. Table 7 further summarises the number of instances where instantaneous energy increase falls below 30 Wh/s or exceeds 200 Wh/s, illustrating extremities of energy deviation among different routes.

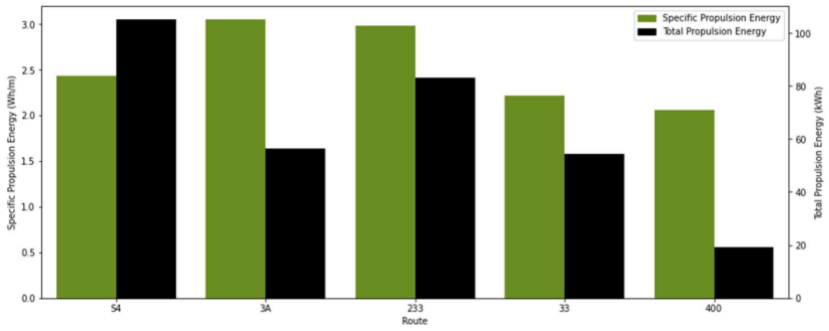

Figure 4: Specific and total propulsion energy consumption for each bus route

Table 7. Summary of instantaneous propulsion energy deviations

Route	Instances where instantaneous energy increase is below 30 Wh/s	Instances where instantaneous energy increase is 30-200 Wh/s	Instances where instantaneous energy increase is above 200 Wh/s
S4	3,680 (83.1%)	711 (16.1%)	38 (0.9%)
3A	3,498 (91.9%)	269 (7.1%)	41 (1.1%)
233	2,005 (75.8%)	599 (22.6%)	42 (1.6%)
33	2,746 (87.8%)	363 (11.6%)	19 (0.6%)
400	1,629 (93.2%)	114 (6.5%)	5 (0.3%)

Overall, there appears to be a broad correlation between the number of high-power instances (above 200 Wh/s) and specific propulsion energy consumption. To determine whether there is any statistically significant relationship between speed and instantaneous energy consumption distributions, the skewness values of both histograms are computed in Figure 5. The Fisher-Pearson correlation coefficient was found to be 0.439, with an R^2 value of 0.193. This suggests that the linear relationship between both distributions' skewness values is slightly positive but weak overall. As such, there are likely to be other influences that affect the energy profiles and overall specific energy consumption – for instance, the number of turns or path geometry.

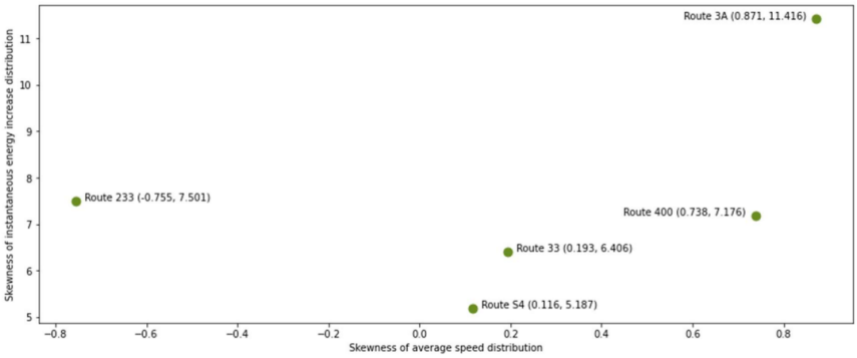

Figure 5: Skewness of speed and energy increase distributions by route

Auxiliary Systems

To apply an energy analysis of auxiliary systems, it was first assumed that all bus fleets would experience high power consumption from non-HVAC auxiliary systems, i.e. $P_{\text{other}} = 3\ kW$. Additionally, air change rates assumed for Oxfordshire were 5 per hour in the winter months, and 9 per hour in the summer months where windows are likely to be open during bus operation. The orifice coefficient k was assumed to be an upper-limit value of 0.6, whilst $V_{\text{passenger}}$ was assumed to be 0.75 by estimating all bus fleets operated with hinged doors. Whilst the rate of boarding η is dependent on passenger demand at each bus stop, an average rate of 5 pax per 20 seconds of bus stopping time was assumed – this gives $\eta = 0.25/s$. Additionally, the number of doors on each bus was taken to be 8, with each door having an estimated area of 3 m^2.

Two temperature conditions were used to simulate both summer and winter demand. As the highest recorded temperature in Oxford was 36.5°C in 2019[36], a hypothetical upper-bound external temperature of 38°C was used, accounting for future weather warming effects. The lowest recorded temperature in Oxford within the last 50 years

[36] R. Lofthouse, "Oxford's Climate Record," Oxford Alumni, Oxford, Jul. 08, 2019.

was -16.6°C in 1982[37] although climate trends in recent years suggest a monthly minimum of 1.9°C[38]; a hypothetical lower-bound external temperature of -5°C was used to reflect that recorded a worst-case scenario and to account for future weather warming effects. The reference internal bus temperature was taken as 22°C for passenger thermal comfort[39], although acknowledging that personal thermal comfort is further affected by variables such as age or clothing insulation. Altogether, this gives $\Delta T_{summer} = 16$°C and $\Delta T_{winter} = 27$°C.

Results for each route are presented for both the worst-case summer and winter conditions in Table 8. The energy consumptions of auxiliary systems were modelled for each bus route, accounting for differences in journey time and time spent with open doors during each stop. In both cases, the power consumption for heating/cooling whilst doors are open represent a significant share of overall energy use, despite the majority of operational time spent travelling with closed doors. This demonstrates the large energy effect of HVAC systems, as well as the direct effect on the number of stops on auxiliary system energy use.

Table 8. Seasonal auxiliary energy consumption during one complete route

Route	Summer Auxiliary Energy Consumption (kWh)	Winter Auxiliary Energy Consumption (kWh)
S4	6.03	6.15
3A	5.02	5.11
233	3.75	3.83
33	4.09	4.17
400	2.07	2.10

Notably, auxiliary energy consumption made up the greatest proportion of total energy consumption in the shortest route 400, at 10.84% and 11.00% during the summer and winter respectively. This suggests that the total energy consumption of shorter routes is more sensitive to changes in auxiliary systems energy use, for instance, due to factors like temperature difference, passenger boarding rates, ventilation and air change rates. As route length increases, overall auxiliary energy consumption also increases monotonically, although the same relationship does not hold true for the proportion of total energy expended on auxiliary systems. This is likely due to total energy consumption, which includes propulsion energy consumption, being influenced by a variety of factors such as route geometry and congestion levels. As such, the SUMO modelling method can provide useful insights into the energy consumption profiles of various routes, thereby highlighting how different route characteristics affect the extent to which auxiliary systems influence overall energy uncertainties.

Conclusion

This study proposed and applied a multi-step process for modelling in-route energy consumption in e-buses, considering both propulsion and auxiliary systems. A multi-criteria decision analysis, combined with analytical hierarchical weighting, was adopted to optimise bus fleet selection based on the route demand and characteristics, including range, charging/refuelling rate, energy storage capacity, and passenger carrying capacity. With the selected bus technical characteristics, road infrastructure was imported from OpenStreetMap into an open-source modelling software SUMO, then edited to input route parameters and geographical bus stop information. In-route propulsion energy consumption was modelled using SUMO, which adopts a white-box theoretical approach to simulate battery energy consumption. Auxiliary energy consumption was modelled separately using a white-box approach, with bus-dependent variables such as air change rates and temperature differences, and route-dependent variables such as stopping duration and overall journey time. Overall, this approach provides a high-level analytical framework for audiences like local authorities and bus operators to understand the energy requirements of different routes, assisting a transition towards zero-carbon fleets.

The proposed methodology was applied in the context of Oxfordshire with 5 selected routes (S4, 3A, 233, 33, and 400) accounting for various operators, route geometries, congestion levels, and servicing regions of high deprivation. Segmenting the routes into two broad categories, two e-buses were selected from the multi-criteria decision process – Mercedez eCitaro G4 for routes S4 and 3A, and Volvo-7900 (18) for routes 233, 33, and 400. Modelling in SUMO showed that propulsion energy consumption ranged from 19.1 kWh to 105 kWh in routes 400 and S4 respectively, with a positive monotonic relationship between route length and overall propulsion energy consumption; plateaus in energy consumption were directly correlated with the extent of congestion experienced. Considering a time-based analysis, the histogram of instantaneous energy increases also differed across routes – the shortest route 400 saw 93.2% and 0.3% of instances observed for changes less than 0.3 kWh and greater than 2 kWh respectively, whilst route 233 saw 75.8% and 1.6% respectively. This suggested strong

[37] S. Burt and T. Burt, "Oxford's Weather and Climate since 1767," Oxford, 2019. Accessed: Jun. 20, 2021. [Online]. Available: https://www.geog.ox.ac.uk/research/climate/rms/oxford-climate.html.
[38] "Oxford climate," Climate-Data.org. https://en.climate-data.org/europe/unitedkingdom/england/oxford-22/ (accessed Jun. 30, 2021).
[39] K. B. Velt and H. A. M. Daanen, "Optimal bus temperature for thermal comfort during a cool day," Applied Ergonomics, vol. 62, pp. 72–76, Jul. 2017, doi: 10.1016/j.apergo.2017.02.014.

correlations between the level of congestion and propulsion energy increase, as non-radial routes were likely to have higher average accelerations. Auxiliary energy modelling showed that energy consumption and the proportion of total energy spent on auxiliary services were correlated more strongly with the number of stops, rather than overall route length, as door-opening significantly affected HVAC loads. Winter consumption was marginally higher than summer, ranging from 2.1 kWh to 6.15 kWh in routes 400 and S4 respectively.

Limitations and Future Work

Several limitations are present in this study and will be discussed in order of approximate influence on overall energy uncertainty. Firstly, elevation data were not considered in this study as SUMO's OpenStreetMap functionality does not allow for the importing of topographic gradient data. The assumption of flat bus routes was considered reasonable as Oxfordshire has a relatively flat topology – the minimum elevation ranges from 52 m in Littlemore to 178 m in central Oxford and Headington[40]. Nevertheless, elevation is often the main factor influencing energy uncertainty in e-buses in practice. Furthermore, this study assumes steady, predictable driving behaviour across all routes. This implies constant acceleration and deceleration rates of $\pm 1.5 m/s^2$, and driving at the constant average speed throughout the journey. In reality, this assumption is untrue both due to traffic elements and inherent driver behaviour. Buses tend to adhere to predetermined schedules, not just by attempting to reach each stop in time but also by stopping for a long period where a destination has been reached too early. Other factors not considered in this modelling were the degradation of the battery, propulsion, and auxiliary systems, variable weight of passengers throughout journeys, as well as the inclusion of other bus geometries such as double-decker e-buses.

To overcome some of the limitations addressed, a robust modelling process should be developed with automated incorporation of elevation data, potentially through satellite or local topographic databases. This can be done in conjunction with powertrain simulation models through platforms like Simulink, which can more specifically examine the influence of propulsion system parameters. To supplement the output of this study, future work can investigate the optimisation of charging infrastructure given the energy consumption profiles of various bus routes. Optimisation of charging infrastructure can also consider other operational factors, including synchronising the required charging sessions with existing bus schedules, waiting times at high-demand bus stops, grid network congestion of local distribution network operators, or marginal costs of laying new grid-connected charging cables.

[40] "Oxfordshire topographic maps," Topographic Map. https://en-gb.topographic-map.com/places/f7/Oxford/ (accessed Jul. 26, 2021).